Published in: *Analytical Letters* **39** (2006) 1721-1734

# ATOMIC FORCE MICROSCOPY CHARACTERISATION OF A MICRO-CONTACT PRINTED, SELF ASSEMBLED THIOL MONOLAYER FOR USE IN BIOSENSORS

D. Caballero, M. Pla-Roca, F. Bessueille, C. A. Mills, J. Samitier and A. Errachid*

Laboratori de Nanobioenginyeria-CREBEC, Parc Científic de Barcelona and Departament d'Electrònica, Universitat de Barcelona, C/ Martí i Franqués, 1 08028-Barcelona, Spain. e-mail:aerrachid@pcb.ub.es, Tel. +34 93 403 71 79, Fax. +34 93 403 71 81.

Published in: *Analytical Letters* **39** (2006) 1721-1734

**Abstract**

This paper describes friction experiments and pull-off force measurements using atomic force microscopy, between a non-functionalised silicon probe and a 2.5 μm diameter $CH_3$ and COOH terminated thiol self assembled monolayer pattern. The pattern is micro-contact printed onto a gold-coated silicon wafer, in air, at room temperature, with a relative humidity around 30%, and used to examine probe-monolayer interactions. Atomic force microscopy imaging reveals that the patterns have been successfully reproduced on the substrate surface. We obtained force values of $(8.67 \pm 2.60)\cdot 10^{-9}$ N, $(2.68 \pm 1.09) \cdot 10^{-8}$ N and $(4.60 \pm 0.24)\cdot 10^{-8}$ N for $CH_3$ terminated alkyl-thiol, COOH terminated thiol and gold substrate respectively. Normalizing these values with the tip radius we obtained (0.87 ± 0.27) N/m for $CH_3$ terminated alkyl-thiol, (2.68 ± 1.10) N/m for COOH terminated thiol and (4.60 ± 2.50) N/m for bare gold. These interactions are discussed in terms of the chemical affinity between the probe and the substrate.

**Keywords:** Micro-contact printing, Self assembled monolayer, Atomic force microscopy.

Published in: *Analytical Letters* **39** (2006) 1721-1734

## 1. Introduction

Atomic force microscopy (AFM) (Binnig and Quate, 1986) is the workhorse for imaging surfaces at nanometric scales. Measurements of adhesion forces at the molecular scale, such as those discussed here, are necessary to understand boundary-layer behaviour through properties such as adhesion and friction (Noy et al., 1995; Fujihira et al., 2001; Tormoen et al., 2004), providing detailed information about the chemistry and the mechanical response of the self-assembled monolayers (SAMs) pattern, and the Au (111) substrate. Friction and adhesion are crucial factors that control the efficiency and durability of the substrate within our final aim building developing a biosensor incorporating such thin films. The development of a number of different measurement modes (Radmacher et al., 1994) has further broadened the field of nanoscale examination of surfaces, be they inorganic- or organic-based, or a mixture of the two. This technique has been particularly helpful in the characterisation of self assembled monolayers on substrate surfaces (Ulman, 1996).

The field of self-assembled monolayers has been extensively examined in the literature (Nuzzo and Allara, 1983; Alves et al., 1992; Ulman, 1996; Christopher et al., 2005). SAMs are molecular assemblies that form spontaneously on a substrate (Widrig et al., 1991). The tail group (SH) of the alkyl-thiol SAM tethers to the gold substrate, with a high S-Au binding energy (E = 48 Kcal/mol) (Dubois and Nuzzo, 1992), in a spontaneous chemisorption process. This contributes to the stability of the SAMs, together with van der Waals (vdW) forces between adjacent methylene groups, and causes the ordering of the alkanethiolate molecules to create the monolayer. The vdW forces are responsible for the tilt angle of the thiol chain from the normal of the Au (111) substrate (Ulman, 1996). The thiols are believed to attach primarily to the threefold hollow sites of the gold surface, forming a $(\sqrt{3}\cdot\sqrt{3})$R30° overlayer structure

(Alves et al., 1992), with a distance between binding sites of 5.0 Å. This results in 21.4 $Å^2$ of available surface area for each molecule. Assuming a vdW diameter for the alkane chain of 4.6 Å (Ulman, 1996), the cross-sectional area of the alkyl chain is much smaller (~16.6 $Å^2$) than the available surface area, causing the chains to tilt to maximize their lateral vdW force. Such SAMs have uses in the biomedical field in the production of biosensors (Davis and Higson, 2004), although in such cases a single continuous film of monolayer is not always desirable. One technique specifically developed to pattern SAMs is that of micro-contact printing (μCP) (Whitesides and Kumar, 1993; Xia and Whitesides, 1998; Christopher et al., 2005) which uses an elastomeric stamp to transfer an "ink" to a suitable substrate where it can be made to self organise in a controlled manner.

Micro-contact printing was first developed by Whitesides and co-workers in 1993 for patterning self-assembled alkanethiol monolayers onto gold substrates (Whitesides and Kumar, 1993). It presents some advantages when compared to other lithographic techniques. It is a fast, simple, and inexpensive technique, requiring no special equipment and can be used to reproduce numerous replicas of a complex pattern from a single mould. The use of elastomeric poly(dimethyl siloxane) (PDMS) stamps also presents a number of advantages (Löttersy et al., 1997). For instance, PDMS is reusable after cleaning; it is durable, non-toxic, chemically inert, and environmentally safe; it deforms reversibly allowing it to conformally contact a substrate; it is optically transparent down to ~300 nm (in the UV-visible region); it has a low thermal expansion; it is hydrophobic (although it can be made temporarily hydrophilic using a plasma treatment); it is permeable to gas (e.g. $CO_2$ and $O_2$); and it can be molded with high fidelity using a mould. However, the main disadvantage of using PDMS for micro-contact printing stamps is that they suffer deformation under pressure due to its inherent

elasticity (Lauera et al., 2001; Hsia et al., 2005) during stamping this can cause expansion of the pattern being printed, and thus, limit the possible resolution.

Micro-contact printed thiol self assembled monolayers are used to modify the properties of the gold substrate, insulating parts of the surface and creating redox-active groups that are the basis for electrochemical biosensors. The synthesis of conducting thiol patterns using self assembled thiol monolayers allow these patterned microstructures to behave like an array of individual microelectrodes. These microelectrodes have several advantages over non-patterned electrodes or traditional ones (Forster, 1994; Stulík et al. 2000; Kudera et al., 2001). Apart from the obvious advantages associated with their reduced size, applicable to small sample volumes or *in vivo* measurements, they are capable of measuring small currents, have small response times, have greatly improved signal-to noise ratios and are useful for low conductivity media (Mrksich and Whitesides, 1995). Furthermore, the pattern acts as a way to precisely control the surface architecture and chemistry. Selective localization of these regions to pattern specific molecules is very important for the development of biosensors, bioMEMS and tissue engineering, for instance.

Using a 2.5 μm diameter, negative PDMS stamp it is possible to obtain a pattern of circular COOH terminated thiol spots that could be used as individual biosensing elements, when used in combination with microelectrodes, surrounded by an isolating $CH_3$ terminated thiol layer. In this work we have used a 2.5 μm diameter positive PDMS stamp to replicate our pattern on the gold substrate, which means the thiol positions are reversed. While this is acceptable for the measurements produced here, in future the pattern will be reversed for integration with the microelectrodes. Friction and adhesion forces were measured to characterise the different chemical interactions between the Si AFM tip and the patterned substrate.

## 2. Materials and methods

### *2.1 Micro-contact printing*

*2.1.1 Mould and substrate preparation*

Micro-contact printing was achieved using transparent, elastomeric polydimethyl siloxane (Sylgard 184, Dow Corning) "stamps", with a patterned relief on one surface. They were replicated from a silicon mould structured by deep reactive ion etching (DRIE) (601 DRIE, Alcatel, France) with circular features 0.8 µm deep.

The mould was first cleaned by submersing in a 50:50 Ethanol:Isobutanol solution (Panreac Química) and then ultrasonicating for ten minutes to remove any PDMS present from previous mouldings. If necessary, the master was further cleaned using Piranha solution (70:30, $H_2SO_4$-$H_2O_2$) (Merck) for 10 minutes. In each case, the mould was thoroughly rinsed several times with deionised water (Milli-Q, 18.2 MΩ·cm resistivity). Finally, the mould was ultrasonicated in fresh deionised water for 2-3 minutes.

The mould was then silanised with a monolayer of Trichlorofluorosilane ($Cl_3FSi$ 153.44 g/mol; Aldrich Chemical Co.). One drop of the silane was placed inside a small vial, and then introduced into a vacuum desiccator with the mould for 1 hour. Prior to use, the mould was rinsed with ethanol (96%) and dried under a $N_2$ flow.

PDMS was prepared by mixing 3 g. of the silicone base polymer with 0.3 g. (10%) of the cross-linking agent. The PDMS stamp was fabricated by placing the mould inside a Petri dish and pouring on the PDMS mixture. The mixture was then placed into a vacuum desiccator for one hour to eliminate any gas bubbles. The Petri dish was then placed in the oven at 90ºC for one hour to cure the polymer. After cooling, the stamp was simply manually demoulded from the mould, ready for use.

Field emission Scanning Electron Microscope (SEM) (S-4100, Hitachi, Japan) and white light interferometry (WYKO NT1100, Veeco Instruments, USA) were used to characterise the 2.5 μm diameter circular pattern on the PDMS stamp surface (Figure 1). The SEM gives us an idea of the fidelity of our stamp with respect the mould (Figure 1a) and the interferometer allows us to obtain a sectional profile of the surface structures in the stamp (Figure 1b). Prior to imaging, the stamp had to be treated, first covering its surface with a few nanometers thick carbon layer by an evaporation process. It was then fixed on the holder with a carbon adhesive tab. Part of the stamp was inked with a silver based-paint to make the polymer conductive and reduce charging.

Substrates of the desired size were cut from Si (100) wafers (Centre Nacional de Microelectrònica CNM, Spain). These substrates were sputter coated with a flat 50 nm gold layer with an ultra high vacuum sputtering system. Before stamping, it was cleaned. First it was placed in a 50:50 Acetone-Tetrahydrofuran (THF) (Panreac Química) mixture and ultrasonicated for 5-10 minutes. It was then dried under a $N_2$ flow and introduced into Piranha solution for 5 minutes giving the surface hydrophilic properties. Finally, it was rinsed with Milli-Q water several times and ultrasonicated in Milli-Q for 5 minutes.

*2.1.2 Thiol preparation and micro-contact printing*

The mould was inked using Octadecanethiol (ODT, $SH(CH_2)_{17}CH_3$; Aldrich Chemical Co.) from a 10 mM solution in ethanol. The stamp was submersed in the thiol for 60 seconds and any excess was removed under a $N_2$ flow for 2-3 minutes. Then the stamp was placed in contact with the gold substrate. A small amount of pressure was applied manually before removing the stamp, leaving the pattern on the substrate. It is important to avoid a prolonged contact time during stamping, because it increases the

risk of ink and contaminant transfer into inter-pattern areas, i.e. by lateral diffusion from the areas where the PDMS stamp is in contact with the substrate. By minimising the contact time, we also avoided ink transmission from the areas of the inked PDMS stamp not in contact with the surface either via the vapour phase. Contamination via the vapour phase of long chain alkyl-thiols is less likely than that by their short chain analogues due to their higher vapour pressures. To repeatedly micro-contact print, the stamp needs only to be inked again with the thiol and repeat the process. Upon completion, the stamp can be cleaned by ultrasonicating with ethanol.

The double $CH_3$ and COOH terminal thiol pattern was achieved immersing the $CH_3$ terminal thiol pattern in a 1 mM of 16-Mercaptohexadecanoic acid (MHA, $SH(CH_2)_{14}COOH$, Aldrich Chemical Co.) in ethanol solution for 12 hours. Finally, the sample was rinsed with ethanol and dried under a $N_2$ flow.

**2.2 Atomic force microscopy characterisation**

A rectangular silicon AFM tip (MikroMasch CSC17/AIBS, spring constant 0.15 N/m, radius of curvature is about 10 nm, aluminium backside coating, 460 μm length) was used for topographical, frictional and adhesional AFM characterisation in air. All images were recorded using a commercial Dimension 3100 AFM (Veeco Instruments, USA) in contact mode. The force measurements were made using a commercial MFP-3D (Asylum Research, USA) atomic force microscope, a microscope specially configured for force measurements.

Pull-off adhesion force measurements were made inside and outside the patterned areas i.e., they were carried out on the functionalised $CH_3$ and COOH terminal thiol areas (as well as on the non-functionalised gold substrate, prior to the double functionalisation) using a non-functionalised silicon AFM tip, also under ambient

conditions. Pull-off force histograms were obtained in order to measure the statistical adhesive force between the different terminal groups.

## 3. Results and discussion

Images of the $CH_3$ terminated thiol SAM pattern, produced by a 2.5 μm diameter PDMS stamp by μCP, are given in Figure 2. As can be clearly seen from this 15 x 15 $\mu m^2$ topography AFM image, the pattern has been successfully reproduced over the gold substrate. The profile of Figure 1b shows that the diameter of the patterned spots agrees with the diameter of the circular features of the PDMS stamp (i.e. 2.5 μm).

Interaction forces were measured between the two functionalised thiol head groups, on the substrate surface, and the non-functionalised silicon AFM tip, under ambient conditions, in air at a relative humidity of 30%. Interaction forces with the pristine gold surface were also measured prior to functionalisation. In Figures 3(a-b) one spot of the pattern can be clearly seen in the topological and friction mode images. A tentative thiol monolayer thickness of 2-4 nm could be measured (Figure 4). Figures 3(c-d) show the patterned $CH_3$ thiol surrounded by the COOH terminated thiol. In this case it is difficult to discern the pattern in topography because the length of the $CH_3$ and COOH terminated thiol is similar. In friction mode it is possible to discern the pattern because of the different adhesion properties, and hence different chemical properties, in the different areas. AFM friction mode microscopy detects changes in the chemical functionality in adjacent regions of patterned SAMs terminated in $CH_3$, COOH terminated thiols and non-functionalised areas. The lateral force between the tip and the substrate increased with the increasing surface tension of the SAM. The morphology of the gold substrate did not significantly modify the pattern of the thiol printed areas as we can see. Contrast between regions of patterned SAMs terminated by $CH_3$ and COOH

groups and bare gold are not significantly influenced by the relative humidity of the atmosphere between 40-60% surrounding the sample (Wilburg et al., 1994), although true humidity effects between the modified tips and the samples are masked by meniscus capillary forces between the tip and the sample due to an adsorbed water layer (Grigg et al., 1992). Thus, we can interpret our results as due to hydrophobic-hydrophilic interactions.

A typical force curve of $CH_3$ terminated thiol patterned area is shown in Figure 5 with a histogram of the data for the pull-off force for 500 measurements. The pull-off measurements were completed to illustrate the different chemical properties of the different patterned areas. The mean pull-off force value is in this case $F = (8.67 \pm 2.60) \cdot 10^{-9}$ *N*, which allows us to calculate the normalized force using the radius of curvature of our probe (R~10 nm), obtaining $F/R = (0.87 \pm 0.27)$ *N/m.* Force measurements were also completed in the COOH terminated thiol region. Figure 6 shows the histogram of the adhesion force values, again for 500. The mean pull-off force value in this case is $F = (2.68 \pm 1.09) \cdot 10^{-8}$ *N*, which gives a normalized force of $F/R = (2.68 \pm 1.10)$ *N/m.*

As previously stated, all the measurements were carried out under ambient conditions and typically there was no specific interaction between the tip and the sample. Under these conditions the SAM surface is coated with a thin layer of adsorbed water and contaminants and therefore a number of precautions must be taken because capillary bridging has been shown to significantly alter the magnitude of the measured adhesion force (Grigg et al., 1992; Wilburg et al., 1994). These species give rise to relatively large capillary forces that can obscure weak intermolecular interactions. The presence of this thin layer of condensed water contacts the tip before it reaches the surface of the SAM (He et al., 2001) and forms a water bridge between the meniscus

and the tip. When the tip retracts the pull-off force is modified. This capillary force, $F_{cap}$, can be expressed simply as:

$$F_{cap} = -4 \cdot \pi \cdot \gamma \cdot R \cdot \cos \theta$$

, where $\gamma$ is the water surface tension ($\gamma = 74.0 \cdot 10^{-3} N/m$), $R$ the tip radius and $\theta$ is the contact angle between the water and the surface. If $\theta = 0$ and $R = 10nm$, then $F_{cap} \sim 10$ $nN$, comparable to the adhesives forces. Therefore, the capillary forces can dominate the "molecular" forces in these measurements. The size of this meniscus and, therefore, the magnitude of the capillary force depends on the relative humidity and the wetting properties of the interacting surfaces. However, despite the presence of this thin water layer, we believe our results to be valid because they show different adhesion values for the different areas, and so, the different chemical properties of the sample.

To compare with the results obtained for the thiol regions, we measured the adhesion force between the silicon tip and the pristine gold (Figure 7). A typical force curve between the gold substrate and the non-functionalised silicon tip is shown, with the histogram of the adhesion forces for 50 measurements. Fewer force measurements were recorded as the gold surface was expected to be more homogeneous. The measured pull-off force was $F = (4.60 \pm 0.24) \cdot 10^{-8}$ $N$ and its normalized value was $F/R = (4.60 \pm 2.50)$ $N/m$. As previously, there is no specific adhesion between the two surfaces, and again a thin layer of water is present during the measurements. The values obtained in this case are mainly due to electrostatic, vdW forces (gold has stronger vdW forces attraction to water than to hydrocarbons) and capillarity forces.

Table 1 gives a summary of all the adhesion force values obtained. Comparing these results we can see that the interaction between the non-functionalised silicon tip and the COOH terminated thiol region is higher than with the $CH_3$ terminated thiol. However, both adhesion forces are lower than the adhesion force value of the pristine

gold. The interaction between two hydrophilic regions, as between the $SiO_2$ of the silicon AFM tip and the COOH terminated thiol region, is stronger than between a hydrophilic region (the Si tip) and a hydrophobic region, such as the $CH_3$ terminated thiol region. The results show that the adhesion decreases as the surface changes from hydrophilic to hydrophobic. As the mean value of each interaction group is outside the standard deviation range of the other interactions, these results show that we can differentiate between chemically distinct functional groups by measuring the adhesion force.

The COOH terminated thiol head group has the potential to act as a molecular recognition centre, as may be appropriate for a biosensor. Modifying this COOH head group with a different (bio)chemistry, it is possible to bind a desired biosensing molecule which specifically binds with the target analyte to be detected. The $CH_3$ terminated thiol head group acts as an isolation layer between the gold substrate and the analyte solution, avoiding non-specific binding of the analyte to the substrate.

We can use the JKR model (Johnson et al., 1971) to estimate the number of molecular interactions contributing to the measured adhesive forces. With a tip radius of ~10 nm, and the cross-sectional area of the alkyl chain being ~16.6 $Å^2$, the contact area at pull-off should correspond to interactions between only a small number of molecules on the surface and the probe tip. Consequently the measurements taken here may give an indication of the kind of values that could be expected for single molecule measurements.

Friction and adhesion force studies in air and liquid media between alkyl-thiol terminal functional groups on an AFM tip and on a gold substrate have been extensively studied. Silicon probes have been coated with $CH_3$ and COOH and gold substrates have been functionalised with similar SAMs (Thomas et al., 1994; Noy et al., 1995; Fujihira

et al., 2001; Tormoen et al., 2004). However, to our knowledge, there are few studies of friction and adhesion force measurements of modified alkyl-thiol SAMs surfaces with *non-functionalised* AFM tips, a technique that precludes the need to functionalise the probe. Functionalising the tip with (hydrophobic) $CH_3$ groups, Tormoen et al. measured an adhesion force value, in air with a relative humidity level of less than 15%, with a $CH_3$ functionalised region of 7.8 nN, a value that is similar to our measured value (8.67 ± 2.60 nN) with a Si tip. The difference is in the hydrophilicity of the $SiO_2$ present on the surface of our tip that gives a higher adhesion value. Noy et al. measured a force value between a COOH/COOH, $CH_3/CH_3$ and $COOH/CH_3$ groups of (2.3 ± 0.4) nN, (1.0 ± 0.4) nN and (0.3 ± 0.2) nN respectively. We show that there is no need to functionalise the tip to be able to distinguish different chemical regions. We have clearly proved that with a commercial non-functionalised silicon tip we are able to distinguish such different regions.

With a new submerged micro-contact printing (SμCP) method (Bessueille et al., 2005), using stamps with aspect ratios unsuitable for conventional μCP, it will be possible to produce well spaced patterned thiol monolayers. Conversion of the COOH into a $NH_2$ group will allow specific binding with a DNA nucleotide. Force measurements between an AFM tip functionalised with the complementary DNA nucleotide and the sample will then be completed to characterise the monolayer for use in a biosensor system.

## 4. Conclusions

A combination of AFM surface topography and friction images, and pull-off force measurements of the patterned thiols have be used for studying the chemical properties of different micropatterned regions of thiols. AFM characterisation, with

respect topography, friction and force characterisation, of these materials is of importance when trying to understand their surface properties and identify different surface species. These measurements have allowed us to discriminate between different areas of micro-contact printed thiol functionalisation, producing average pull-off force values for each area using a standard silicon AFM probe. Such micro-contact printed monolayers can be used to form the basis for biosensors, as further functionalisation of the thiol can be undertaken to add biological functionality in specific areas. Here we report the fabrication and characterisation of well-defined micropatterns within a single step based on the microcontact printing technique technique. The interactions presented are to be used as the basis for studying the force interactions between a modified thiol and a DNA functionalised AFM probe, for use in a biosensor system. This approach will impact on both fundamental research and development of electrochemical sensor devices.

**Acknowledgement**

This work has been supported by the Spanish government MEC (Ministerio de Educación y Ciencia) through the projects PCI 76/03-04, HF2005-0055, NAN2004-09415-C05-01 and TEC2005-07996-C02-021MIC. The authors wish to acknowledge Dr. E. Martínez from Nanotechnology Platform of Barcelona Science Park for her helpful and insightful comments concerning this subject.

**References:**

Alves, C.A., E.L. Smith and M.D. Porter. 1992. Atomic scale imaging of alkanethiolate monolayers at gold surfaces with atomic force microscopy. *J. Am. Chem. Soc.* 114: 1222-1227.

Bessueille, F., M. Pla-Roca, C.A. Mills, E. Martínez, J. Samitier and A. Errachid. 2005. Submerged micro-contact printing (SμCP): an unconventional printing technique of thiols using high aspect ratios, elastomeric stamps. *Langmuir*. 21: 12060-12063.

Binnig, G. and C.F. Quate. 1986. Atomic force microscope. *Phys. Rev. Lett.* 56, 9: 930-933.

Christopher, J., L.A. Estroff, J.K. Kriebel, R.G. Nuzzo and G.M. Whitesides. 2005. Self-assembled monolayers of thiolates on metals as a form of nanotechnology. *Chem. Rev*. 105: 1103-1169.

Davis, F. and S.P.J. Higson. 2004. Structured thin films as functional components within biosensors. *Biosens. Bioelectr.* 21: 1-20.

Dubois, L.H. and R.G. Nuzzo. 1992. Synthesis, structure, and properties of model organic surfaces. *Ann. Rev. Phys. Chem.* 43: 437-463.

Forster, R.J. 1994. Microelectrodes: new dimensions in electrochemistry. *Chem. Soc. Rev*. 23: 289-297.

Fujihira, M., M. Furugori, U. Akiba and Y. Tani. 2001. Study of microcontact printed patterns by chemical force microscopy. *Ultramicroscopy.* 86: 75-83.

Grigg, D.A., P.E. Russel and J.E. Griffith. 1992. Tip-sample forces in scanning probe microscopy in air and vacuum. *J. Vac. Sci. Tech. A.* 10: 680-683.

He, M., A. S. Blum, D. E. Alston, C. Buenviaje and R.M. Overney. 2001. Critical phenomena of water bridges in nanoasperity contacts. *J. Chem. Phys.* 114: 1355-1360.

Hsia, K. J., Y. Huang, E. Menard, J.U. Park, W. Zhou, J. Rogers and J.M. Fulton. 2005. Collapse of stamps for soft lithography due to interfacial adhesion. *Appl. Phys. Lett.* 86: 154106.

Johnson, K.L., K. Kendall and A.D. Roberts. 1971. Surface energy and contact of elastic solids. *Proc. R. Soc. London, A.* 324: 301-321.

Kudera, M., O. Allen, H. Hill, P.J Dobson, P.A. Leigh and W.S. McIntire. 2001. Electrochemical characterisation and application of multi microelectrode array devices to biological electrochemistry. *Sensors*. 1: 18-28.

Lauera, L., C. Klein and A. Offenhaüsser. 2001. Spot compliant neuronal networks by structure optimized micro-contact printing. *Biomaterials.* 22: 1925-1932.

Löttersy, J.C., W. Olthuis, P.H. Veltink and P. Bergveld. 1997. The mechanical properties of the rubber elastic polymer polydimethylsiloxane for sensor applications. *J. Micromech. Microeng*. 7: 145–147.

Mrksich, M. and G.M. Whitesides. 1995. Patterning self-assembled monolayers using microcontact printing: a new technology for biosensors? *Trends in Biotech*. 13, 6: 228-235.

Noy, A., C.D. Frisbie, L.F. Rozsnyai, M.S. Wrighton and C.H. Lieber. 1995. Chemical force microscopy: exploiting chemically-modified tips to quantify adhesion, friction, and functional group distributions in molecular assemblies. *J. Am. Chem. Soc.* 117: 7943-7951.

Nuzzo, R.G. and D.L. Allara. 1983. Adsorption of bifunctional organic disulfides on gold surfaces. *J. Am. Chem. Soc.* 105, 13: 4481-4483.

Radmacher, M., J.P. Cleveland, M. Fritz, H.G. Hansma and P.K. Hansma. 1994. Mapping interaction forces with the atomic force microscope. *Biophys. J.* 66: 2159-2165.

Stulík, K., C. Amatore, K. Holub, V. Marecek and W. Kutner. 2000. Microelectrodes. Definitions, characterization, and applications. *Pure App. Chem*. 72, 8: 1483-1492.

Thomas, R.C., J.E. Houston, R.M. Crooks, T. Kim and T.A. Michalske. 1995. Probing adhesion forces at the molecular scale. *J. Am. Chem. Soc.* 117: 3830-3834.

Tormoen, G.W., J. Drelich and E.R. Beach. 2004. Analysis of atomic force microscope pull-off forces for gold surfaces portraying nanoscale roughness and specific chemical functionality. *J. Adhesion Sci. Technol*. 18, 1: 1-17.

Ulman, A. 1996. Formation and structure of self-assembled monolayers. *Chem. Rev.* 96: 1533-1554.

Whitesides, G.M. and A. Kumar. 1993. Features of gold having micrometer to centimeter dimensions can be formed through a combination of stamping with an elastomeric stamp and an alkanethiol "ink" followed by chemical etching. *Appl. Phys. Lett.* 63, 14: 2002-2004.

Widrig, C.A., C.A. Alves and M.D. Porter. 1991. Scanning tunneling microscopy of ethanethiolate and n-octadecanethiolate monolayers spontaneously absorbed at gold surfaces, *J. Am. Chem. Soc*. 113: 2805-2810.

Wilburg, J.L., H.A. Biebuyck, J.C. MacDonald and G.M. Whitesides. 1994. Scanning force microscopies can image patterned self-assembled monolayers. *Langmuir*. 11: 825-831.

Xia, Y. and G.M. Whitesides. 1998. Soft lithography. *Angew. Chem. Int. Ed.* 37: 550-575.

Published in: *Analytical Letters* **39** (2006) 1721-1734

**Figure/Table captions**

**Fig 1** (a) SEM image of one of the structural features on the PDMS stamp used for micro-contact printing and, inset, an array of the features from the stamp. (b) Sectional profile of the surface structures of the stamp.

**Fig 2** AFM topography image of micro-contact printed $CH_3$ terminated thiol pattern acting which could be used in conjunction with a microelectrode array for electrochemical measurements.

**Fig 3** AFM images of micro-contact printed thiol patterns, successfully reproduced over the gold substrate. (a) Topographical and (b) friction mode AFM images of the patterned gold surface. (c) Topographic and (d) friction mode AFM images of the patterned $CH_3$ terminated thiol surrounded by the COOH terminated thiol. It is difficult to discern differences in the topographical image due to the similarity in chain length of the two thiols.

**Fig 4** AFM topography cross sectional profile of the $CH_3$ terminated thiol patternshowing a SAM thickness of approximately 2-4 nm.

**Fig 5** Histogram of the pull-off force data for 500 measurements between the $CH_3$ terminal thiol region and the non-functionalised Si AFM tip. Inset, a typical force curve.

**Fig 6** Histogram of the pull-off force data for 500 measurements between the COOH terminal thiol region and the non-functionalised Si AFM tip. Inset, a typical force curve.

**Fig 7** Histogram of the pull-off force data for 50 measurements between the pristine gold substrate and the non-functionalised Si AFM. Inset, a typical force curve.

**Table 1** Summary table of statistics of the adhesion force measurements *(F)* and the normalized ones *(F/R)* with their standard desviation $\Delta$.

Published in: *Analytical Letters* **39** (2006) 1721-1734

Figure 1 (Caballero et al.)

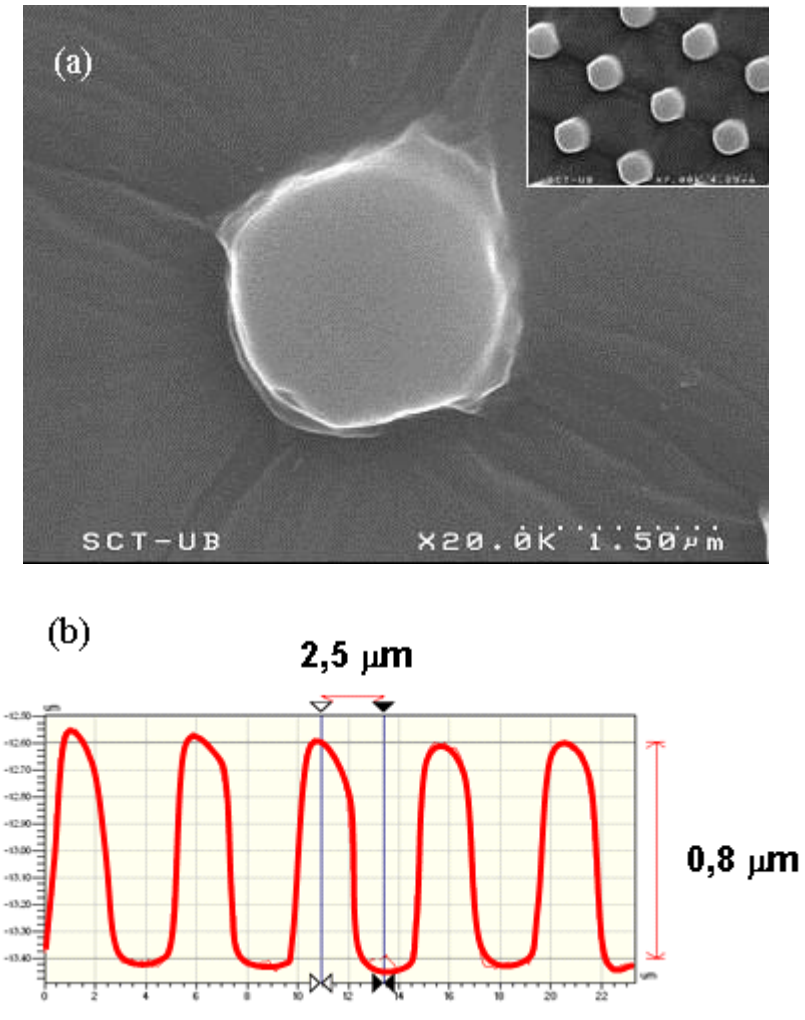

Published in: *Analytical Letters* **39** (2006) 1721-1734

Figure 2 (Caballero et al.)

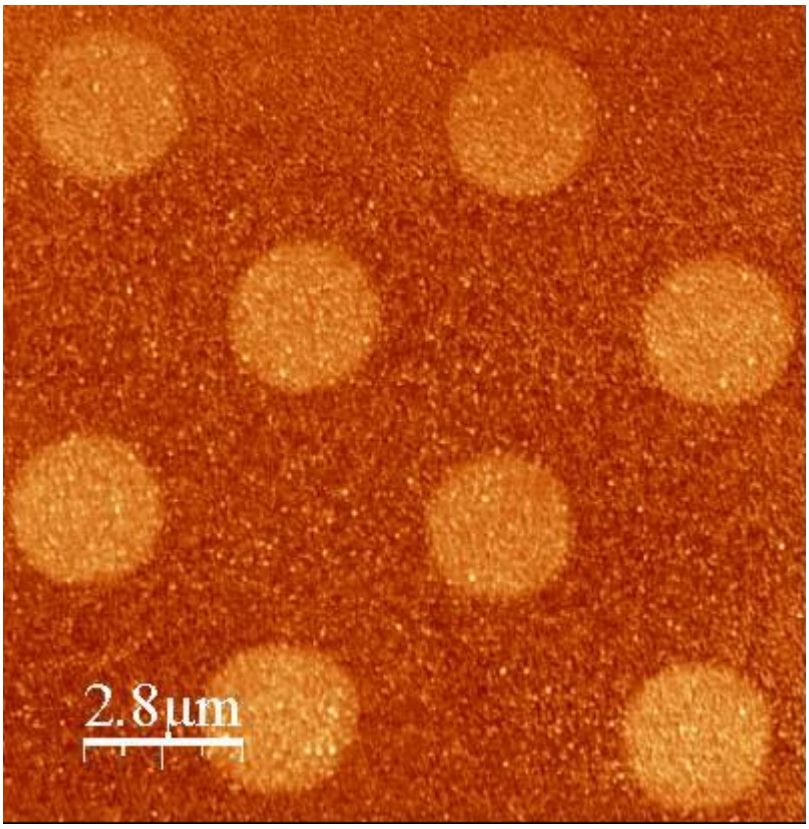

Published in: *Analytical Letters* **39** (2006) 1721-1734

Figure 3 (Caballero et al.)

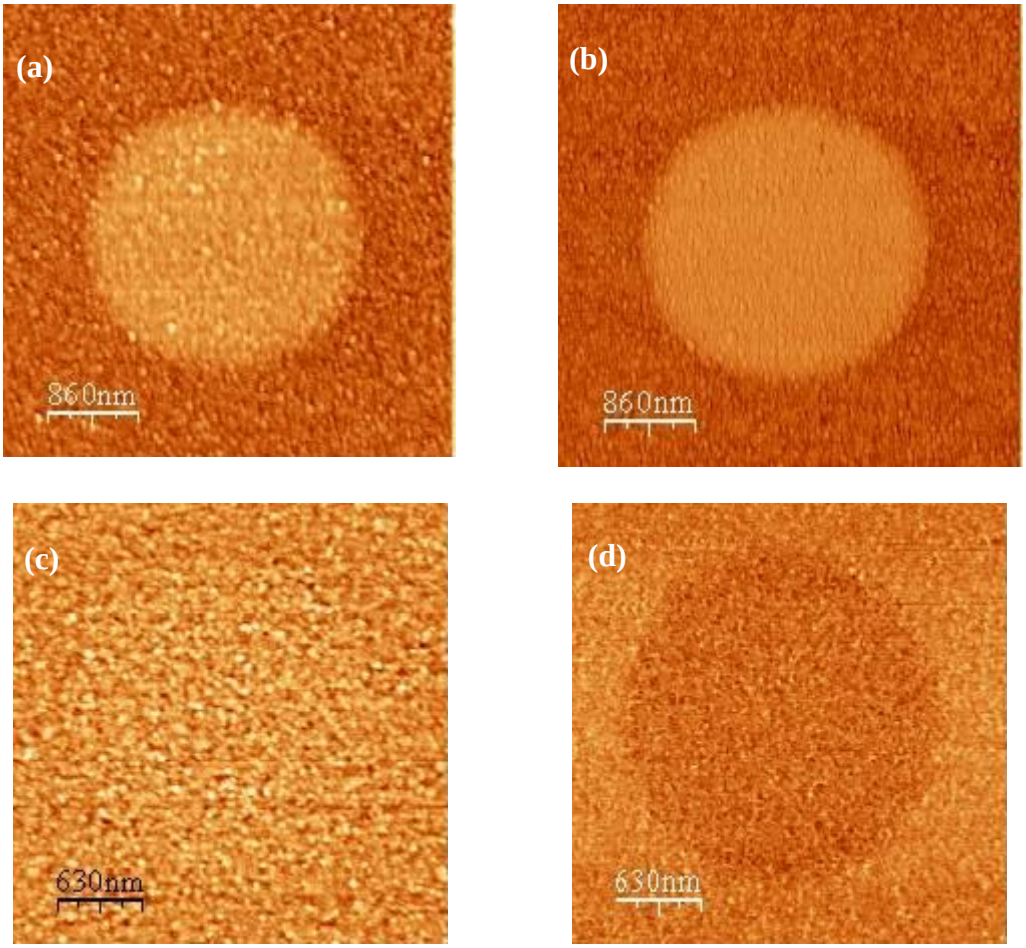

Published in: *Analytical Letters* **39** (2006) 1721-1734

Figure 4 (Caballero et al.)

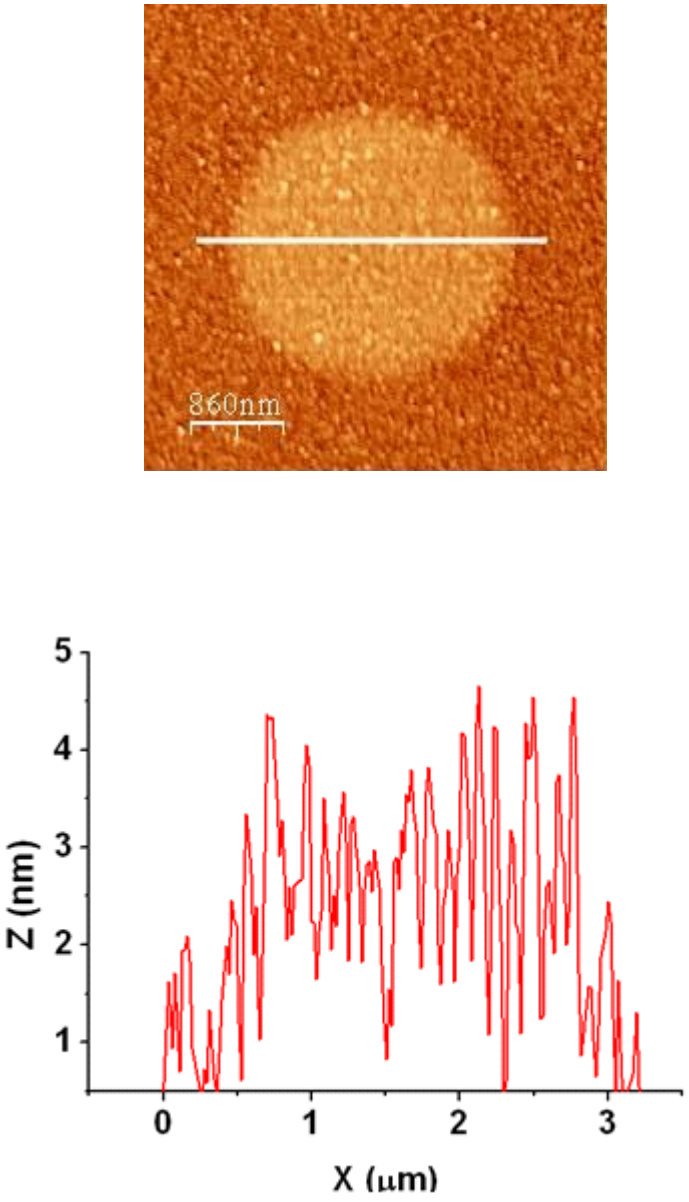

Published in: *Analytical Letters* **39** (2006) 1721-1734

Figure 5 (Caballero et al.)

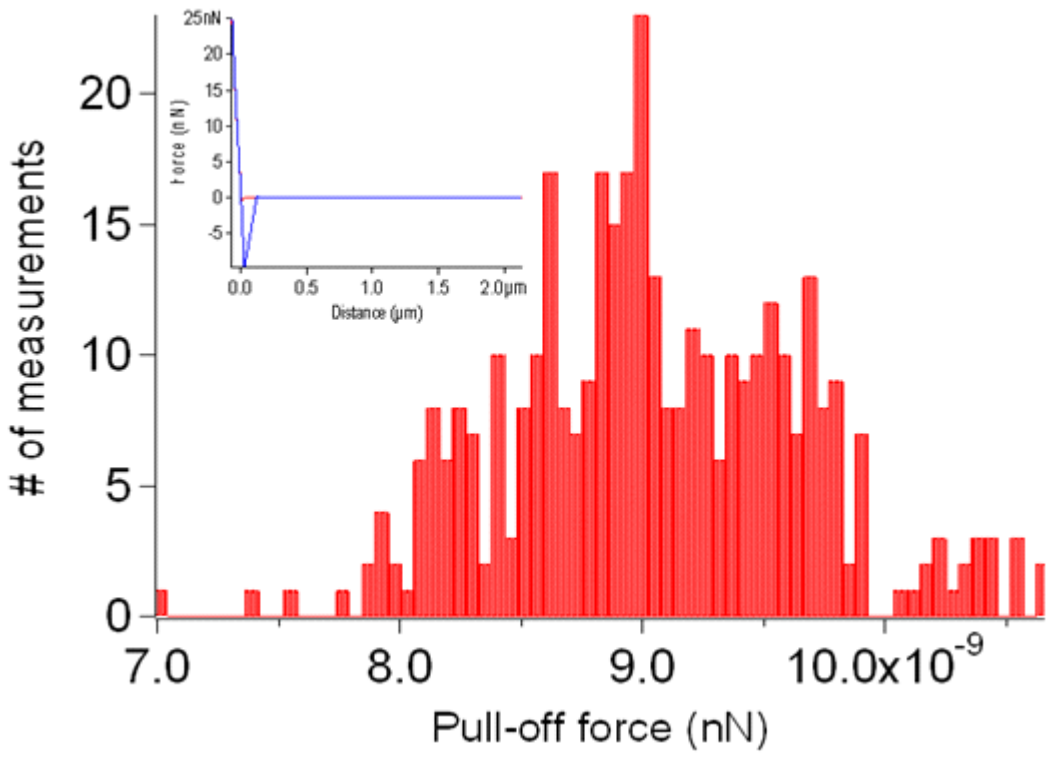

Published in: *Analytical Letters* **39** (2006) 1721-1734

Figure 6 (Caballero et al.)

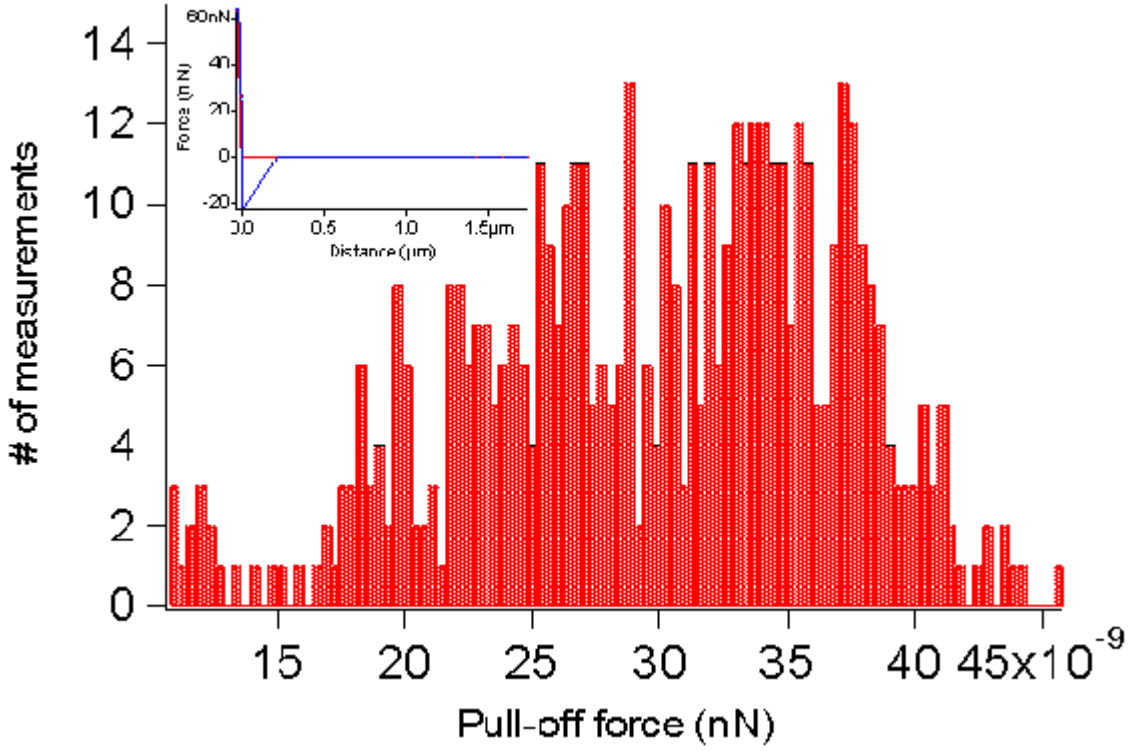

Published in: *Analytical Letters* **39** (2006) 1721-1734

Figure 7 (Caballero et al.)

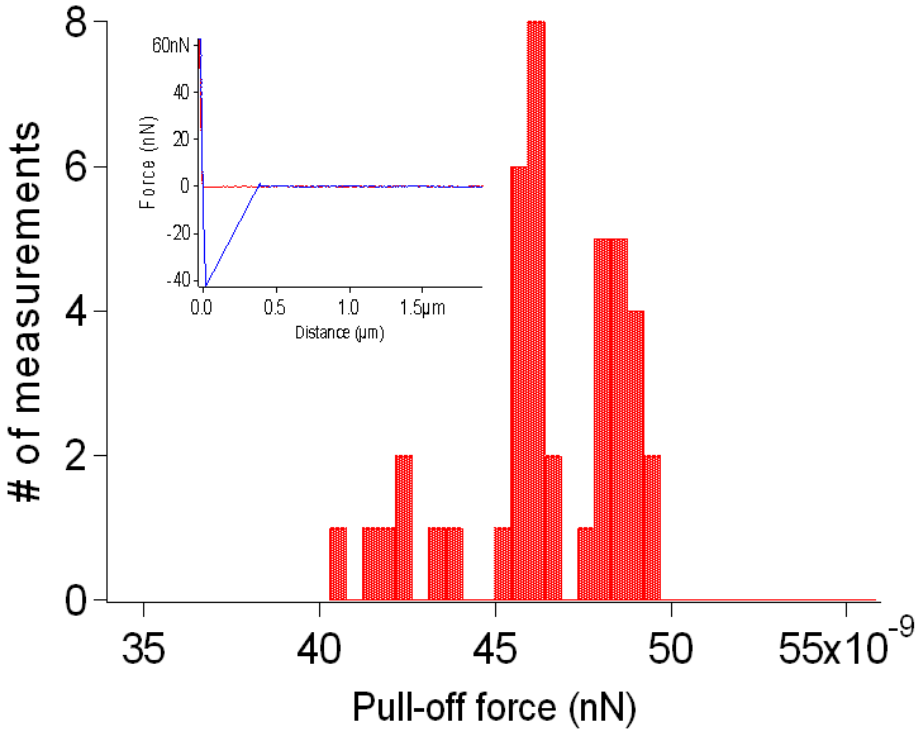

Published in: *Analytical Letters* **39** (2006) 1721-1734

Table 1 (Caballero et al.)

| | **F (N)** | **ΔF (N)** | **F/R (N/m)** | **ΔF/R (N/m)** |
|---|---|---|---|---|
| **Si vs $CH_3$** | $8.67 \cdot 10^{-9}$ | $2.60 \cdot 10^{-9}$ | *0.87* | *0.27* |
| **Si vs COOH** | $2.68 \cdot 10^{-8}$ | $1.09 \cdot 10^{-8}$ | *2.68* | *1.10* |
| **Si vs Au** | $4.60 \cdot 10^{-8}$ | $0.24 \cdot 10^{-8}$ | *4.6* | *2.50* |